Closed-Form Shock Solutions

B. M. Johnson

December 12, 2013

Disclaimer

This document was prepared as an account of work sponsored by an agency of the United States government. Neither the United States government nor Lawrence Livermore National Security, LLC, nor any of their employees makes any warranty, expressed or implied, or assumes any legal liability or responsibility for the accuracy, completeness, or usefulness of any information, apparatus, product, or process disclosed, or represents that its use would not infringe privately owned rights. Reference herein to any specific commercial product, process, or service by trade name, trademark, manufacturer, or otherwise does not necessarily constitute or imply its endorsement, recommendation, or favoring by the United States government or Lawrence Livermore National Security, LLC. The views and opinions of authors expressed herein do not necessarily state or reflect those of the United States government or Lawrence Livermore National Security, LLC, and shall not be used for advertising or product endorsement purposes.

Closed-form shock solutions

B. M. Johnson[1]†

[1]Lawrence Livermore National Laboratory, Livermore, CA 94550, USA

It is shown here that a subset of the implicit analytical shock solutions discovered by Becker and by Johnson can be inverted, yielding several exact, closed-form solutions of the one-dimensional, compressible Navier-Stokes equations for an ideal gas. For a constant dynamic viscosity and/or thermal conductivity, and at particular values of the shock Mach number, the velocity can be expressed in terms of a polynomial root. For a constant kinematic viscosity, independent of Mach number, the velocity can be expressed in terms of a hyperbolic tangent function. The remaining fluid variables are related to the velocity through simple algebraic expressions. The solutions derived here make excellent verification tests for numerical algorithms, since no source terms in the evolution equations are approximated, and the closed-form expressions are straightforward to implement. The solutions are also of some academic interest as they may provide insight into the non-linear character of the Navier-Stokes equations.

Key words:

---

1. Introduction

One of the few known non-linear analytical solutions to the equations of fluid dynamics was discovered by Becker (1922) and subsequently analyzed by Thomas (1944), Morduchow & Libby (1949), Hayes (1960) and Iannelli (2013). It captures the physical profile of shock fronts in ideal gases, and although it requires some restrictive assumptions (a steady-state, one planar dimension, constant dynamic viscosity, an ideal gas equation of state, and a constant Prandtl number Pr of 3/4), the solution is exact in the sense that no source terms in the (one-dimensional) evolution equations are neglected or approximated. Analogous solutions were discovered by Johnson (2013) in the limit of both large and small Pr. These solutions provide a useful framework for verifying numerical algorithms used to solve the Navier-Stokes equations. A drawback, however, from the perspective of both physical intuition and numerical implementation, is that the solutions are implicit, i.e., they are solutions for $x(v)$ rather than closed-form expressions for $v(x)$ (x here is the spatial dimension in which the shock propagates and v is the velocity in that direction).

It is shown here that some of these implicit solutions can be inverted for particular values of the shock Mach number, yielding closed-form expressions for the fluid velocity as a function of position. In particular, for rational values of the shock compression ratio, Becker's implicit expression is a polynomial in $v(x)$. Expressions for the polynomial root relevant to a shock are provided up to a compression ratio of four. Polynomial solutions also exist in both the large and small Pr limits under the assumption of either a constant dynamic viscosity or constant thermal conductivity, and expressions are provided for these as well. Under the assumption of a constant kinematic (rather than dynamic)

† Email address for correspondence: johnson359@llnl.gov

viscosity, the solution for $v(x)$ takes the particularly simple form of a hyperbolic tangent function; this solution is valid at any Mach number and for both $Pr \to \infty$ and $Pr \to 3/4$.

An overview of the equations to be solved are given in §2, the solutions are given in §3, and a summary is given in §4.

2. Equations

In one planar dimension and a steady-state, the compressible Navier-Stokes equations reduce to the following ordinary differential equations:

$$\frac{4\mu}{3m_0}v\frac{dv}{dx} = v^2 + \frac{\gamma - 1}{\gamma}h - \frac{\gamma + 1}{2\gamma}\left(v_0 + v_1\right)v, \tag{2.1}$$

$$\frac{\kappa}{m_0 C_p}\frac{dh}{dx} = \frac{h}{\gamma} - \frac{v^2}{2} + \frac{\gamma + 1}{2\gamma}\left(v_0 + v_1\right)v - \frac{\gamma + 1}{\gamma - 1}\frac{v_0 v_1}{2}, \tag{2.2}$$

where ρ is the mass density, v is the velocity magnitude in the x direction, $h = e + p/\rho$ is the fluid enthalpy, p is the pressure, e is the internal energy, μ is the dynamic viscosity (in the limit of negligible bulk viscosity; otherwise μ is the sum of the dynamic viscosity and $3/4$ the bulk viscosity), κ is the thermal conductivity and $m_0 = \rho v = \rho_0 v_0$ is the mass flux (Becker 1922; Zel'dovich & Raizer 2002; Johnson 2013). It has been assumed here that the fluid obeys an ideal gas equation of state, $p = (\gamma - 1)\rho e$, so that $h = \gamma e = C_p T$, where C_p is the specific heat at constant pressure, T is the temperature, and $\gamma = C_p/C_v$ is the adiabatic index (C_v is the specific heat at constant volume). The integration constants in equations (2.1) and (2.2) have been expressed in terms of both pre-shock (denoted by a subscript "0") and post-shock (denoted by a subscript "1") velocities using the shock compression ratio:

$$R \equiv \frac{\rho_1}{\rho_0} = \frac{\gamma + 1}{\gamma - 1 + 2/M_0^2}, \tag{2.3}$$

where $M_0^2 = v_0^2/c_0^2$ is the shock Mach number and $c_0 = \sqrt{\gamma p_0/\rho_0}$ is the adiabatic sound speed in the ambient fluid (Landau & Lifshitz 1987). The Prandtl number is given by $Pr \equiv \mu C_p/\kappa$.

3. Solutions

3.1. *Becker ($Pr = 3/4$) solution*

For $Pr = 3/4$, equations (2.1) and (2.2) can be reduced to the quadrature (Becker 1922)

$$x = \frac{2L_\kappa}{\gamma + 1}\int \frac{(\kappa/\kappa_0)\,\eta}{(\eta - 1)(\eta - \eta_1)}\,d\eta, \tag{3.1}$$
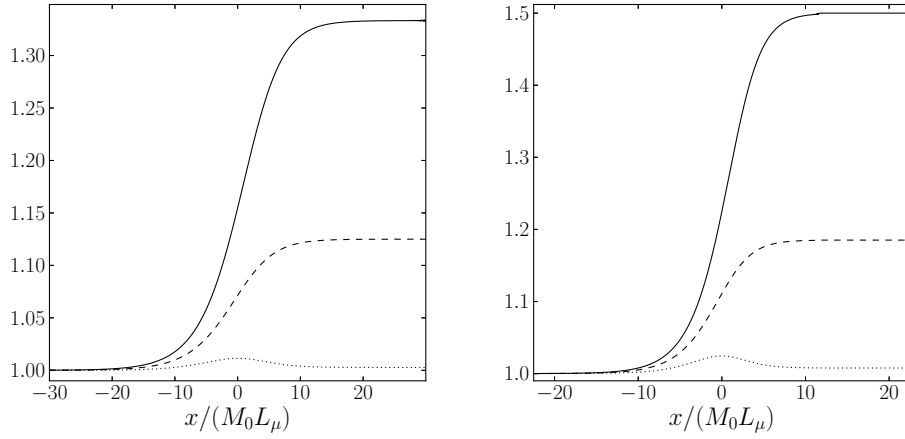
and the algebraic expression

$$\frac{T}{T_0} = \frac{\gamma - 1}{2}M_0^2\left(\frac{\gamma + 1}{\gamma - 1}\eta_1 - \eta^2\right). \tag{3.2}$$

Here $\eta \equiv v/v_0$, $\eta_1 \equiv v_1/v_0 = R^{-1}$, and $L_\kappa \equiv \kappa_0/(m_0 C_v)$ is the ambient conductive length scale. For constant $\kappa = \kappa_0$, the integral (3.1) is given by (to within an arbitrary constant)

$$x = \frac{2L_\kappa}{\gamma + 1}\ln\left[(1 - \eta)^{\frac{1}{1 - \eta_1}}(\eta - \eta_1)^{-\frac{\eta_1}{1 - \eta_1}}\right], \tag{3.3}$$

R	M_0^2	Equation
4/3	$8/(7-\gamma)$	$\delta^4 - f\left(\delta^3 + 3\delta^2/4 + 3\delta/16 + 1/64\right) = 0$
3/2	$6/(5-\gamma)$	$\delta^3 + f\left(\delta^2 + 2\delta/3 + 1/9\right) = 0$
2	$4/(3-\gamma)$	$\delta^2 - f\left(\delta + 1/2\right) = 0$
3	$3/(2-\gamma)$	$\delta^3 + f^2\left(\delta + 2/3\right) = 0$
4	$8/(5-3\gamma)$	$\delta^4 - f^3\left(\delta + 3/4\right) = 0$

TABLE 1. $Pr = 3/4$ and $Pr = \infty$ polynomials

FIGURE 1. Curves of density (*solid*), temperature (*dashed*) and a proxy for the entropy (*dotted*) for $Pr = 3/4$ solutions with $R = 4/3$ (*left*) and $R = 3/2$ (*right*).

which is in turn equivalent to

$$(\delta - \delta_1)\, f^{R-1} = (-\delta)^R, \tag{3.4}$$

where $\delta \equiv \eta - 1$, $\delta_1 \equiv \eta_1 - 1 = R^{-1} - 1$,

$$f \equiv e^{x/w}, \tag{3.5}$$

and

$$w \equiv \frac{2L}{\gamma + 1}. \tag{3.6}$$

Here $L = L_\kappa$, but expression (3.6) is kept general for use in later sections.

For rational values of R, equation (3.4) is a polynomial in $\delta(x)$. Values for R that yield closed-form expressions for $v(x)$ are listed in table 1, the corresponding closed-form expressions for η are given in the appendix, and plots of the density, temperature and a proxy for the entropy ($s \equiv T\eta^{\gamma-1}$) are shown in figures 1–3. Plotted quantities are all normalized to their ambient values, and the x-values have been scaled to $M_0 L_\mu$ ($= M_0 L_\kappa/\gamma$ for $Pr = 3/4$), as this is a length scale that is independent of the shock Mach number. Table 1 also gives the curves in M_0–γ space for which the closed-form solutions are valid. These can be obtained by solving expression (2.3) for M_0:

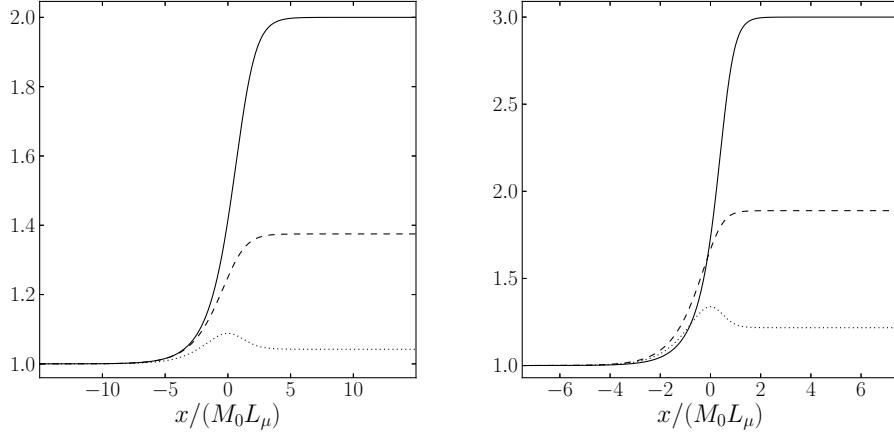$$M_0 = \sqrt{\frac{2R}{R + 1 - \gamma(R - 1)}} \tag{3.7}$$

FIGURE 2. Curves of density (*solid*), temperature (*dashed*) and a proxy for the entropy (*dotted*) for $Pr = 3/4$ solutions with $R = 2$ (*left*) and $R = 3$ (*right*).
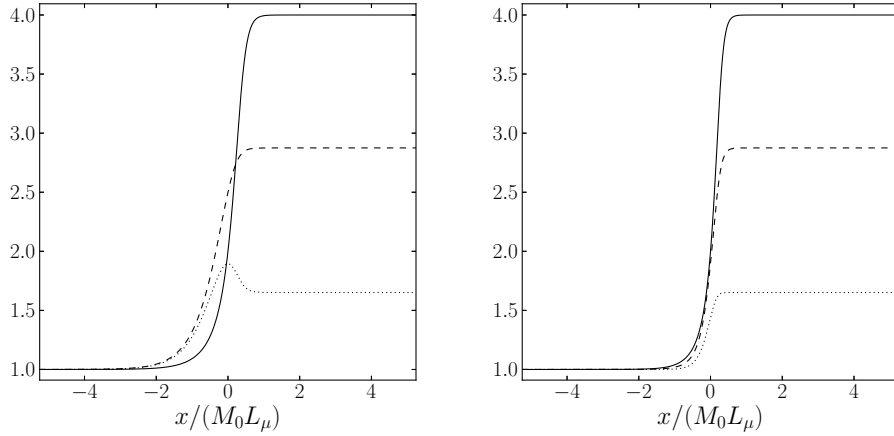

FIGURE 3. Curves of density (*solid*), temperature (*dashed*) and a proxy for the entropy (*dotted*) for a $Pr = 3/4$ solution (*left*) and a $Pr = \infty$ solution (*right*) with $R = 4$.

3.2. *Large-Pr solution*

For $Pr \rightarrow \infty$, equations (2.1) and (2.2) can be reduced to the quadrature (Johnson 2013)

$$x = \frac{2L_\mu}{\gamma + 1} \int \frac{(\mu/\mu_0)\,\eta}{(\eta - 1)\,(\eta - \eta_1)}\, d\eta, \tag{3.8}$$

where $L_\mu \equiv 4\mu_0/(3m_0)$ is the ambient viscous length scale, and the algebraic expression

$$T = T_0 \frac{\gamma(\gamma - 1)M_0^2}{2} \left(\eta^2 - 4\eta_i\eta + \frac{\gamma + 1}{\gamma - 1}\eta_1 \right), \tag{3.9}$$

where

$$\eta_i \equiv \frac{\gamma + 1}{4\gamma}\left(1 + \eta_1\right). \tag{3.10}$$

For constant $\mu = \mu_0$, the integral (3.8) is given by (to within an arbitrary constant)

$$x = \frac{2L_\mu}{\gamma + 1} \ln \left[(1 - \eta)^{\frac{1}{1 - \eta_1}} (\eta - \eta_1)^{-\frac{\eta_1}{1 - \eta_1}} \right]. \tag{3.11}$$

Comparing expression (3.11) with (3.3), it can be seen that the solutions for η in this limit are the same as those of the previous section with $L = L_\mu$ in expression (3.6). Figure 3 compares the large-Pr solution with $R = 4$ to the corresponding $Pr = 3/4$ solution. Notice that the entropy has no local maximum in this limit (it increases monotonically from pre- to post-shock). This can be seen from

$$\frac{d\ln T}{dx} + (\gamma - 1)\frac{d\ln \eta}{dx} = 0 \rightarrow \eta^2 - (1 + \eta_1)\,\eta + \eta_1 = 0, \tag{3.12}$$

which is solved by $\eta = 1$ and $\eta = \eta_1$; the entropy has zero slope only at the boundaries.

3.3. *Small-Pr solution*

For $Pr \to 0$, equations (2.1) and (2.2) can be reduced to the quadrature (Johnson 2013)

$$x = \frac{4L_\kappa}{\gamma + 1} \int \frac{(\kappa/\kappa_0)\,(\eta - \eta_i)}{(\eta - 1)\,(\eta - \eta_1)}\, d\eta, \tag{3.13}$$

and the algebraic expression

$$T = T_0 \gamma M_0^2 \eta \left(2\eta_i - \eta\right). \tag{3.14}$$

For constant $\kappa = \kappa_0$, the integral (3.13) is given by (to within an arbitrary constant)

$$x = \frac{4L_\kappa}{\gamma + 1} \ln \left[(1 - \eta)^{\frac{1 - \eta_i}{1 - \eta_1}} (\eta - \eta_1)^{\frac{\eta_i - \eta_1}{1 - \eta_1}} \right], \tag{3.15}$$

which is in turn equivalent to

$$f^{|n-1|/2}\,(\delta - \delta_1) = (-\delta)^n, \tag{3.16}$$

where

$$n \equiv \frac{\eta_i - 1}{\eta_i - \eta_1} = \frac{(\gamma + 1)(1 - \gamma M_0^2)}{1 - 3\gamma + (3 - \gamma)\gamma M_0^2}, \tag{3.17}$$

f is defined in expression (3.5), and $L = L_\kappa$ in expression (3.6). For $M_0^2 > 1$, $1 < |n| < \infty$.

For rational values of n, equation (3.16) is a polynomial in $\delta(x)$. Values for n that yield closed-form expressions for $v(x)$ are listed in table 2, the corresponding closed-form expressions for η are given in the appendix, and plots of the density, temperature and a proxy for the entropy are shown in figures 4–7. Plotted quantities are again normalized to their ambient values, and the x-values have been scaled to $M_0 L_\kappa$. Table 2 also gives the curves in M_0–γ space for which the closed-form solutions are valid. These can be obtained by solving expression (3.17) for M_0:

$$M_0 = \sqrt{\frac{\alpha\gamma - 1}{\gamma(\alpha - \gamma)}}, \quad \alpha \equiv \frac{3n + 1}{n - 1}. \tag{3.18}$$

In terms of α,

$$\delta_1 = -2\frac{\gamma - 1}{\alpha\gamma - 1}. \tag{3.19}$$

For $M_0 > M_c$, where

$$M_c \equiv \sqrt{\frac{3\gamma - 1}{\gamma\,(3 - \gamma)}} \tag{3.20}$$

(this is equivalent to $\alpha < 3$ or $n < 0$), the solution in this limit is discontinuous (Zel'dovich & Raizer 2002; Johnson 2013). For $M_0 = M_c$, $n = \pm\infty$, $\eta_i = \eta_1$, and equation (3.16) reduces to $f^{1/2} = -\delta$, or $\eta = 1 - f^{1/2}$. This solution is valid until $\eta = \eta_1$, where there
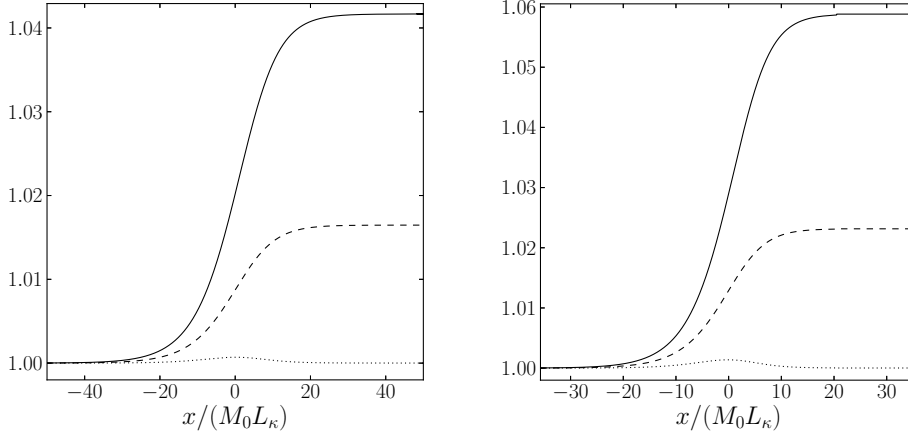
FIGURE 4. Curves of density (*solid*), temperature (*dashed*) and a proxy for the entropy (*dotted*) for $Pr = 0$ solutions with $n = 4/3$ (*left*) and $n = 3/2$ (*right*).
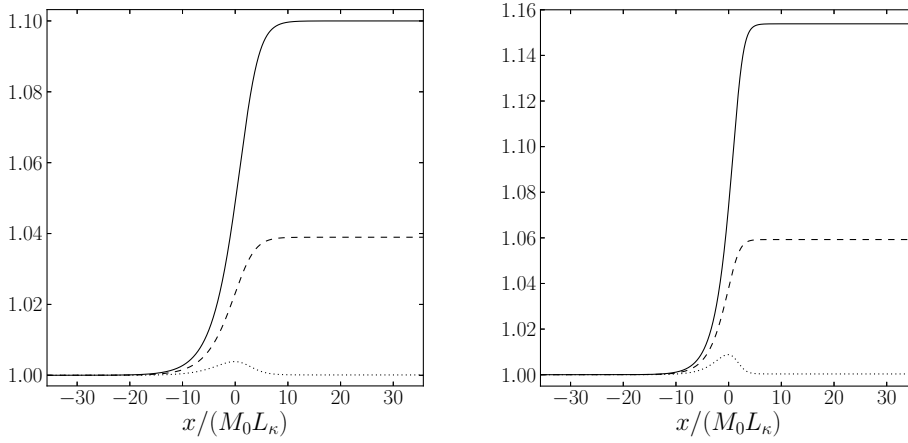

FIGURE 5. Curves of density (*solid*), temperature (*dashed*) and a proxy for the entropy (*dotted*) for $Pr = 0$ solutions with $n = 2$ (*left*) and $n = 3$ (*right*).

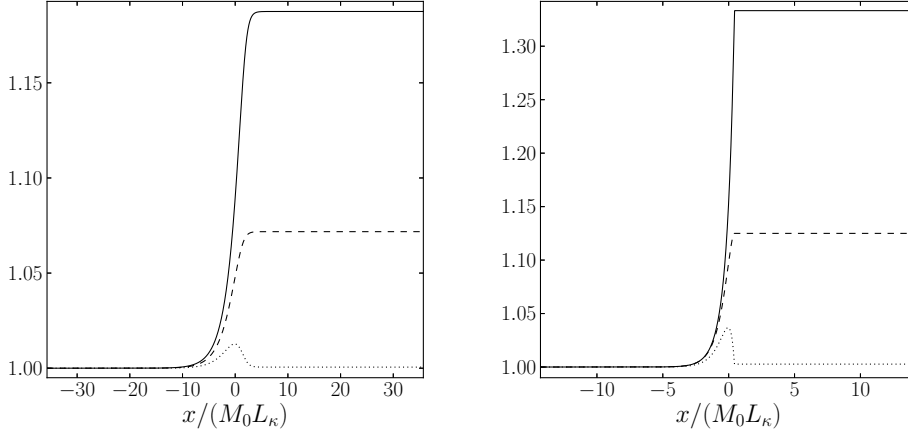| n	α	M_0^2	Equation
-3	2	$(2\gamma - 1)/(\gamma[2 - \gamma])$	$\delta^4 - \delta_1\delta^3 + f^2 = 0$
-2	5/3	$(5\gamma - 3)/(\gamma[5 - 3\gamma])$	$\delta^3 - \delta_1\delta^2 - f^{3/2} = 0$
4/3	15	$(15\gamma - 1)/(\gamma[15 - \gamma])$	$\delta^4 + f^{1/2}\left(-\delta^3 + 3\delta_1\delta^2 - 3\delta_1^2\delta + \delta_1^3\right) = 0$
3/2	11	$(11\gamma - 1)/(\gamma[11 - \gamma])$	$\delta^3 + f^{1/2}\left(\delta^2 - 2\delta_1\delta + \delta_1^2\right) = 0$
2	7	$(7\gamma - 1)/(\gamma[7 - \gamma])$	$\delta^2 + f^{1/2}\left(-\delta + \delta_1\right) = 0$
3	5	$(5\gamma - 1)/(\gamma[5 - \gamma])$	$\delta^3 + f\left(\delta - \delta_1\right) = 0$
4	13/3	$(13\gamma - 3)/(\gamma[13 - 3\gamma])$	$\delta^4 + f^{3/2}\left(-\delta + \delta_1\right) = 0$
∞	3	$(3\gamma - 1)/(\gamma[3 - \gamma])$	$\delta + f^{1/2} = 0$

TABLE 2. $Pr = 0$ polynomials

FIGURE 6. Curves of density (*solid*), temperature (*dashed*) and a proxy for the entropy (*dotted*) for $Pr = 0$ solutions with $n = 4$ (*left*) and $n = \infty$ (*right*).
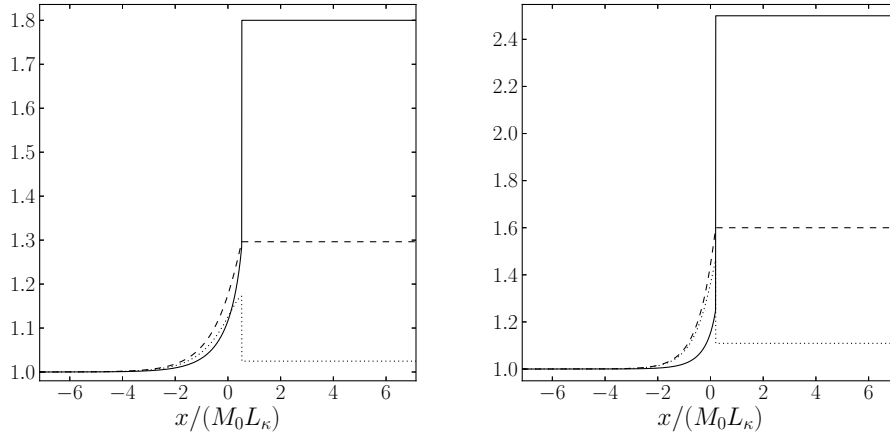

FIGURE 7. Curves of density (*solid*), temperature (*dashed*) and a proxy for the entropy (*dotted*) for $Pr = 0$ solutions with $n = -3$ (*left*) and $n = -2$ (*right*).

is a weak discontinuity in both velocity and temperature. The weak discontinuity in the temperature occurs above the first derivative, since $dT/dx \propto \eta_i - \eta = 0$ at $\eta = \eta_i$.

3.4. *Constant kinematic viscosity*

For a constant kinematic viscosity, $\nu \equiv \mu/\rho = \nu_0$, the integrals (3.1) and (3.8) both reduce to

$$x = w \int \frac{d\eta}{(\eta - 1)(\eta - \eta_1)} = \frac{w}{1 - \eta_1} \ln\left(\frac{1 - \eta}{\eta - \eta_1}\right), \tag{3.21}$$

which can be solved for η to give

$$\eta = \sigma(-z) + \eta_1 \, \sigma(z), \tag{3.22}$$

where

$$\sigma(z) \equiv \frac{1}{1 + e^{-z}}, \quad z \equiv \frac{x}{w}(1 - \eta_1) = \frac{x}{L}\left(1 - M_0^{-2}\right).$$
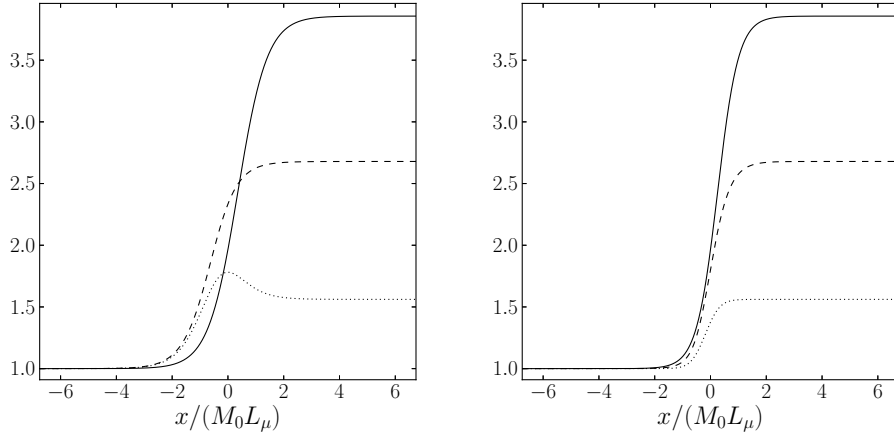
FIGURE 8. Curves of density (*solid*), temperature (*dashed*) and a proxy for the entropy (*dotted*) for a $Pr = 3/4$ solution (*left*) and a $Pr = \infty$ solution (*right*) with constant ν and $M_0 = 3$.

An equivalent expression for η is

$$\eta = \frac{\eta_1 + 1}{2} + \frac{\eta_1 - 1}{2}\tanh\left(\frac{z}{2}\right). \tag{3.23}$$

This solution is valid for both $Pr = 3/4$, in which case $L = L_\kappa = \gamma L_\mu$ and T is given by expression (3.2), and $Pr = \infty$, in which case $L = L_\mu$ and T is given by expression (3.9). Plots of the density, temperature and a proxy for the entropy (normalized to their ambient values) are shown in figure 8 for both $Pr = 3/4$ and $Pr = \infty$.

4. Summary

Several closed-form analytical solutions to the one-dimensional compressible Navier-Stokes equations have been derived in the limit of a steady-state and an ideal-gas equation of state. Solutions with a constant dynamic viscosity and/or thermal conductivity can be obtained by solving a polynomial equation. Polynomial solutions valid for large Pr and $Pr = 3/4$ are listed in table 1 and shown in figures 1–3. Polynomial solutions valid for small Pr and listed in table 2 and shown in figures 4–7. Tables 1 and 2 also give expressions for $M_0(\gamma)$ for which these solutions are valid, and the corresponding curves in M_0–γ space are shown in figure 9. A solution can also be obtained under the assumption of a constant kinematic viscosity, valid for either large Pr or a constant $Pr = 3/4$ and at any Mach number; this solution is described in §3.4 and shown in figure 8.

The derived solutions are non-linear and exact in the sense that no source terms in the evolution equations are neglected or approximated. As such, they make excellent verification tests for numerical algorithms. The solutions may also provide insight into the non-linear character of the Navier-Stokes equations. The solution set is not exhaustive, as additional polynomial solutions exist under the assumption of a constant thermal diffusivity $\chi \equiv \kappa/\rho$, and a solution in terms of Lambert functions can be derived for $\mu \propto T^{1/2}$, $Pr \to \infty$ and $M_0 \to \infty$. As none of these solutions are more physically-relevant than the ones discussed above, their detailed derivation has not been included.
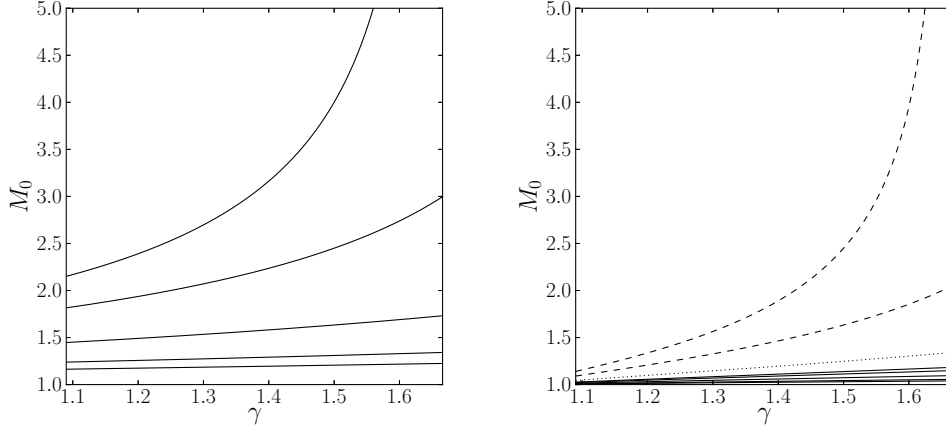
FIGURE 9. Curves in M_0–γ space for which the derived closed-form solutions are valid, for $R = 4/3$, 3/2, 2, 3 and 4 (*left, bottom to top*), and for $n = -3$, -2, ∞, 4/3, 3/2, 2, 3 and 4 (*right, top to bottom*). On the right, a dashed line indicates a discontinuous solution, a dotted line indicates a solution with a weak discontinuity, and a solid line indicates a continuous solution.

Appendix A

For the quadratic equations in tables 1 and 2 ($\delta^2 + a\delta + b = 0$), the solution branch relevant to a shock (the other solution branch grows exponentially as $x \to \infty$) is given by

$$\eta = 1 - \frac{a}{2} - \sqrt{\left(\frac{a}{2}\right)^2 - b}. \tag{A 1}$$

For the cubic equations in tables 1 and 2 ($\delta^3 + a\delta^2 + b\delta + c = 0$), the shock solution is

$$\eta = 1 - \left(\frac{a}{3} + A + \frac{p}{A}\right), \tag{A 2}$$

where

$$A \equiv \left(q + \sqrt{q^2 - p^3}\right)^{\frac{1}{3}}, \quad p \equiv \left(\frac{a}{3}\right)^2 - \frac{b}{3}, \quad q \equiv \left(\frac{a}{3}\right)^3 - \frac{ab}{6} + \frac{c}{2}.$$

For $R = 3/2$ and $n = 3/2$, the solution is given by expression (A 2) for $f < f_c$, where f_c is given in table 3, and by

$$\eta = 1 + 2\sqrt{p}\cos\left(\frac{\theta - 2\pi k}{3}\right) - \frac{a}{3}, \quad \theta \equiv \cos^{-1}\left(\frac{-q}{p^{3/2}}\right) \tag{A 3}$$

for $f > f_c$ (with $k = 0$). For $n = -2$, the solution is given by expression (A 3) for $f < f_c$ (with $k = 1$), and there is a discontinuity at $f = f_c$ where the solution transitions from $2\eta_i - \eta_1$ to η_1 (Zel'dovich & Raizer 2002; Johnson 2013). Evaluating expression (A 3) can be problematic as $x \to \infty$ due to the subtraction of two large numbers that are nearly equal. This can be seen in the right panel of figures 1 and 4, where a glitch in the density appears near the post-shock region. The data for these plots (generated with `numpy`) was noisy beyond this point and was replaced with post-shock values at infinity.

For the quartic equations in tables 1 and 2 ($\delta^4 + a\delta^3 + b\delta^2 + c\delta + d = 0$), the shock solution is

$$\eta = 1 - \frac{a}{4} + \frac{k}{2}B - \frac{k}{2}\sqrt{-B^2 + 3r - s\frac{k}{B}}, \tag{A 4}$$

Solution	k	f_c
$R = 4/3$	1	
$R = 3/2$	0	$9/4$
$R = 4$	1	
$n = -3$	-1	$\left(\delta_1 \delta_i^3 - \delta_i^4\right)^{1/2}$
$n = -2$	1	$\left(\delta_i^3 - \delta_1 \delta_i^2\right)^{2/3}$
$n = 4/3$	1	
$n = 3/2$	0	$\left(27\delta_1/4\right)^2$
$n = 4$	1	
$n = \infty$		$-\delta_1$

TABLE 3. Branches and critical points

where

$$A \equiv \left(q + \sqrt{q^2 - p^3}\right)^{\frac{1}{3}}, \quad B \equiv \sqrt{r + A + \frac{p}{A}},$$

$$p \equiv \left(\frac{b}{3}\right)^2 - \frac{ac}{3} + \frac{4d}{3}, \quad q \equiv \left(\frac{b}{3}\right)^3 - \frac{abc}{6} + \frac{a^2 d}{2} + \frac{c^2}{2} - \frac{4bd}{3},$$

$$r \equiv \left(\frac{a}{2}\right)^2 - \frac{2}{3}b, \quad s \equiv \frac{a^3}{4} - ab + 2c,$$

and the value for k is given in table 3. For $n = -3$, there is a discontinuity at $f = f_c$ where the solution transitions from $2\eta_i - \eta_1$ to η_1 (Zel'dovich & Raizer 2002; Johnson 2013).

The translational invariance of the equations allows one to multiply f by any constant factor. To set the origin $x = 0$ at $\eta = \eta_o$, where $\eta_1 < \eta_o < 1$ but is otherwise arbitrary, multiply f by a scale factor S, where S is obtained from the relevant equation. For example, the equation for $R = 2$ with $f \to Sf$ is

$$\delta^2 - Sf\left(\delta + 1/2\right) = 0.$$

Since $f = 1$ at $x = 0$, this equation can be solved for S to give

$$S = \frac{\delta_o^2}{\delta_o + 1/2},$$

where $\delta_o = \eta_o - 1$.

REFERENCES

BECKER, R. 1922 Stosswelle und Detonation. *Z. Physik.* **8**, 321–362.

HAYES, W. D. 1960 *Gasdynamic Discontinuities*. Princeton University Press.

IANNELLI, J. 2013 An exact non-linear Navier-Stokes compressible-flow solution for CFD code verification. *Int. J. Numer. Meth. Fl.* **72**, 157–176.

JOHNSON, B. M. 2013 Analytical shock solutions at large and small Prandtl number. *J. Fluid Mech.* **726**, 4.

LANDAU, L. D. & LIFSHITZ, E. M. 1987 *Fluid Mechanics*. Butterworth–Heinemann.

MORDUCHOW, M. & LIBBY, P. A. 1949 On a complete solution of the one-dimensional flow equations of a viscous, heat conducting, compressible gas. *J. Aeron. Sci.* **16**, 674–684.

THOMAS, L. H. 1944 Note on Becker's theory of the shock front. *J. Chem. Phys.* **12**, 449–452.

ZEL'DOVICH, YA. B. & RAIZER, YU. P. 2002 *Physics of Shock Waves and High-Temperature Hydrodynamic Phenomena*. Dover.